On the Structural Perspective of Computational Effectiveness for Quantized Consensus in Layered UAV Networks

Yan Wan, *Senior Member, IEEE*, Jing Yan, *Member, IEEE*, Zongli Lin, *Fellow, IEEE*, Vardhman Sheth, and Sajal K. Das, *Fellow, IEEE*

***Abstract*—Distributed computing tasks in small unmanned aerial vehicle (UAV) networks require effective data transmission schemes because of limited communication channels and transmission power. In this paper, we use distributed consensus as a canonical distributed computing task to study the effectiveness of the data transmission in digitized (quantized) channels for UAV networks. We show that layered structures are more effective than equivalent egalitarian structures in terms of the data transmission load required to reach consensus. In particular, we establish explicit relationships between simple structural characteristics and the performance of quantized consensus (e.g., consensus condition, consensus value, and transmission load to reach consensus) for broad classes of layered structures. We also provide analytical results on asymptotic and transient performance when additional local memories are used to further reduce the data transmission load to reach consensus.**

***Index Terms*—Consensus, layered networks, quantization, unmanned aerial vehicle (UAV) networks.**

I. Introduction

With the advent of unmanned aerial vehicle (UAV) technologies and recent release of new small UAV rules by the Federal Aviation Administration [1], UAVs have increasingly been used as a cost-effective and flexible sensing and computational platform for a variety of civilian applications. For instance, UAVs can collaboratively stitch real-time videos to increase the area of surveillance coverage [2]. Similarly, UAVs can share loads to collaboratively monitor fires, measure air quality, or trace chemical leakages with optimized performance in terms of traveling time, data transmission latency, and coverage (see, e.g., [3]).

Effective communication and data transmission are critical for distributed UAV computing applications. Different from ground-based computing platforms, which are typically less constrained by various resources, distributed UAV computation faces several new challenges. First, there is the *digitalized data transmission*. A realistic UAV communication network uses digital links of limited channel data rates. Data need to be quantized and coded before transmission. This quantization procedure introduces nonlinearity to the distributed computing tasks. Second is the challenge of *limited availability of communication channels*. We cannot expect a UAV network of dense communication links among agents, which are more likely to be affected by channel inferences. Third is the *limited transmission power* challenge. Small payloads and limited power supplies of UAVs limit their wireless data transmission capabilities [4], [5]. Fourth is the challenge of *network management for moving UAVs*. Hierarchical structures are easier for network management tasks [6].

Existing works on distributed control typically focus on stability and time efficiency issues, but do not consider communication issues such as transmission load. Ideal communication links are often assumed without considering inference, limited channel data rates, and transmission power constraints. In this paper, we use distributed consensus, a canonical distributed computing task, in a UAV network to study the effectiveness of data transmission for cooperative UAV computation. From a structural perspective, we quantitatively connect the network topology to the performance of distributed computation, in terms of the transmission load needed to reach consensus.

Distributed consensus is generally concerned with a group of agents of different initial opinions converging to the same opinion through *local* communication among neighbors. It is a typical distributed computing task in sensor networks, and has been widely studied in the control theory literature (see, e.g., [7]–[9]). Most of these studies assume "egalitarian" networks of the following properties: 1) agents are of the same functionality and no organization or hierarchy exists among these egalitarian agents, 2) the data from neighbors are immediately transmitted and available at any time instance.

Manuscript received January 6, 2018; accepted February 18, 2018. Date of publication March 8, 2018; date of current version March 14, 2019. This work was supported by the National Science Foundation under Grant CAREER-1714519 and Grant CRI-1730675. Recommended by Associate Editor Y. Hong. This paper was presented in part at the IEEE International Conference on Distributed Computing in Sensor Systems, Marina Del Rey, CA, USA, May 26–28, 2014 [35]. *(Corresponding author: Yan Wan.)*

Y. Wan is with the Department of Electrical Engineering, University of Texas at Arlington, Arlington, TX 76019 USA (e-mail: yan.wan@uta.edu).

J. Yan is with the Department of Electrica Engineering, Yanshan University, Qinhuangdao 066004, China (e-mail: yanjing6663@163.com).

Z. Lin is with the Charles L. Brown Department of Electrical and Computer Engineering, University of Virginia, Charlottesville, VA 22904 USA (e-mail: zl5y@virginia.edu).

V. Sheth is with Linear Dimensions Semiconductor Inc, San Jose, CA 95123 USA (e-mail: vardhmansheth@my.unt.edu).

S. K. Das is with the Department of Computer Science, Missouri University of Science and Technology, Rolla, MO 65409 USA (e-mail: sdas@mst.edu).

Digital Object Identifier 10.1109/TCNS.2018.2813926

By noticing that such egalitarian structures are not efficient with respect to transmission load, we study in this paper nonegalitarian structures where agents take different roles. In [10], we analyzed layered networks of a multilayer multigroup (MLMG) topology and communication scheme, and established the precise connection between such a layered structure and the consensus performance, such as a consensus condition, the final consensus value, and the consensus time. In this paper, we find that such a structure can be significantly more effective in terms of the transmission load to reach consensus, compared to equivalent egalitarian networks. In addition, Wan *et al.* [10] focused on linear deterministic dynamics of perfect communication channels, and this paper extends the analysis to stochastic nonlinear quantized consensus for digitized channels of limited data rates. Furthermore, we find in this paper that additional local memories can further be employed to reduce the transmission load. This property makes MLMG structures suitable for UAV networks, which require sparse data transmissions. Layered structures have been widely used in practical sensor networks, which have demonstrated the advantages of both high energy efficiency and network management simplicity [11], [12]. However, sparse efforts have been made on the performance analysis and systematic design of these nonegalitarian networks from a control's perspective (see, e.g., [13]).

The main contributions of this paper are summarized as follows.

1) *Quantized consensus in MLMG networks of limited data rates:* Quantized consensus has been studied in symmetric egalitarian networks, characterized by doubly stochastic system matrices. Our characterizations of the asymptotic and transient performance of quantized consensus contribute to the literature in that: a) the network's equivalent egalitarian structure is asymmetric and not doubly stochastic, and b) we directly relate simple topological characteristics of MLMG networks with the quantized consensus performance.
2) *Characterization of the efficiency of MLMG structures for UAV networks:* The MLMG communication structure lies between centralized and egalitarian distributed structures. It maintains the features of distributed communication globally, while reducing the number of transmissions to reach consensus compared to egalitarian distributed networks of the same dynamics. The reduction in the transmission load is calculated, and is shown to grow quadratically with the size of the network, suggesting the high efficiency of the MLMG structures in large-scale UAV networks and beyond.
3) *Characterization of the structural impact on the consensus performance:* The MLMG structures are interesting in that they capture hidden topological information that is not observable in the egalitarian structures directly associated with the consensus dynamics. They provide simple topological characteristics that lead to explicit graphical results on consensus performance, such as consensus condition, consensus value, consensus rate, and transmission load. These graphical results are very useful in large-scale network applications as they permit scalable network designs.
4) *Memory-based quantization scheme design:* We introduce additional local memories to UAVs to further reduce the transmission load, and study the asymptotic and transient properties of quantized consensus in MLMG networks. This design is motivated by increasing correlations among transmitted values along the consensus process. We show that the employment of additional memories can significantly further reduce the transmission load in terms of the number of bits transmitted to reach consensus.

This paper is organized as follows. In Section II, we describe the MLMG structure and communication scheme, probabilistic quantization, and consensus dynamics with/without the employment of additional local memories. In Section III, we study the asymptotic and transient consensus properties when the probabilistic quantization scheme is adopted for digital channels of limited data rates. In Section IV, we explicitly relate the characteristics of the network structure with the number of transmissions to reach consensus for broad classes of MLMG structures. In Section V, performance analysis is extended to the case when additional local memory is introduced. Section VI describes the simulation studies. Finally Section VII concludes this paper.

II. Modeling Framework

A. Layered MLMG Topology

Consider a layered UAV network of n nodes: 1) m *fusion centers* (FCs) at higher layers, serving as *group leaders* with the full functionality of sensing, fusion, and communication, and 2) $n-m$ *sensor nodes* at the bottom layer with the functionality of sensing, simple local computation, and communication to FCs. Links between sensor nodes and FCs represent communication channels. MLMG networks can have multiple layers, forming hierarchical networks as discussed in [10]. In this paper, we focus on the two-layer multigroup (2LMG) structures, with the understanding that many results can be generalized to networks of more than two layers. Fig. 1(a) shows a two-layer two-group (2L2G) structure where $m=2$ and $n=6$. Group 1 includes FC_1, sensor nodes S_2 and S_3, and group 2 includes FC_2, S_5, and S_6.

To facilitate structural analysis, we separate the sensing and fusion functionalities of each FC to a *leader sensor node* and a *virtual fusion center* (VFC), which is deprived of the sensing capability. With that, the 2LMG network topology is rearranged to a network of $n+m$ nodes (represented by bipartite graph $\mathcal{G}$), where sensor nodes are indexed by S_i, $i \in \{1,2,\ldots,n\}$, and VFCs are indexed by VFC_j, $j \in \{1,2,\ldots,m\}$. As an example, the VFC version of Fig. 1(a) is as shown in Fig. 1(b). VFC_1 communicates with every sensor node in its group and also S_4 in the other group. Similarly, VFC_2 communicates with every sensor node in its group and also S_1 in the other group. We use a matrix $H \in \mathcal{R}^{m\times n}$ to capture the network topology. In particular, in the *MLMG topology matrix* $H \in R^{m\times n}$, each entry (i,j) is "1" if sensor node j is connected to VFC i, and "0"

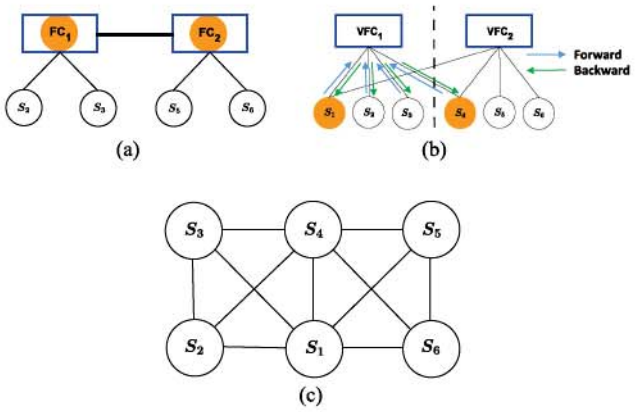

Fig. 1. Example of the 2L2G structure. (a) Topology graph with FCs at the top layer and sensor nodes at the bottom layer. (b) VFC version. (c) Equivalent egalitarian network of the same consensus dynamics.

otherwise. For the 2L2G example shown in Fig. 1, we have $H = \begin{bmatrix} 1 & 1 & 1 & 1 & 0 & 0 \\ 1 & 0 & 0 & 1 & 1 & 1 \end{bmatrix}$. The number of communication links that a VFC (or sensor) is connected to is called the *degree* of the VFC (or sensor). A 2LMG network is *regular* if all VFCs are of the same degree, denoted as r. A *path* is a sequence of communication links that connect the VFCs and the sensor nodes.

B. Forward and Backward Communication Scheme

The communication in MLMG networks is featured by the *forward and backward operations*typically observed in centralized networks. Specifically, the following steps are involved in each iteration of consensus [see Fig. 1(b)]:

1) in the forward step, each sensor node sends its value to the VFC, which it connects to;
2) each VFC updates with the average of connected sensor values, and then in the backward step sends its value to these sensor nodes; and
3) each sensor node updates with the average of connected VFC values.

This forward and backward communication scheme is very different from the purely distributed communication scheme for a network of egalitarian agents, where at each iteration, every node fuses sensor values immediately available from neighboring nodes.

The MLMG structures with the forward and backward communication scheme demonstrate features of both centralized and distributed communication structures. In particular, they maintain distributed communication across groups, but use centralized forward and backward communication scheme within each group. Centralized structures (with all sensor nodes communicating with a single leader using forward and backward communications) are effective with the minimum number of data transmissions, but are not practical in large-scale networks due to a variety of issues such as the vulnerability to attacks, data traffic bottlenecks at base stations, the lack of flexibility, and the incapability to scale. In contrast, distributed structures, widely studied in the control community, achieve better performance in terms of security, throughput, flexibility and scalability, but at the cost of a significantly larger number of transmissions to reach consensus. In a related vein, Su and Gamal in [14] compared the number of rounds and the network rate distortion function between the centralized and the distributed structures for gossip consensus algorithms. The MLMG structures, which reside between centralized and distributed structures, serve as a means for us to understand the tradeoffs between these two extreme structures to meet UAV networking needs.

C. MLMG Network Dynamics

The aforementioned forward and backward operations at each iteration k can be described by the following dynamics:

$$\mathbf{x}[k+1] = A\mathbf{x}[k] = K_1 H^T K_2 H \mathbf{x}[k] \tag{1}$$

where $\mathbf{x}[k]$ is sensor values at k, $K_1 = [\text{diag}(H^T \mathbf{1}_{m\times 1})]^{-1}$, $K_2 = [\text{diag}(H\mathbf{1}_{n\times 1})]^{-1}$, $A \in \mathcal{R}^{n\times n}$ is the *system matrix*, and diag( ) places a vector's entries in a diagonal form.

Matrix A defines a graph structure, $\tilde{\mathcal{G}}$, of an *egalitarian distributed network*, which has the same dynamics as that of the 2LMG structure defined on H. The egalitarian distributed network of Fig. 1(b) defined by matrix A is shown in Fig. 1(c), where each entry $A_{i,j} \neq 0$ if sensor node i receives data from sensor node j through a VFC in each iteration. The MLMG structures expose hidden structures that are not directly observable in egalitarian distributed networks, and hence, provide a new structural approach to obtaining tractable graph-theoretic results on consensus properties.

D. Dynamics for MLMG Networks of Digitalized Channels

To account for digital channels of limited data rates, quantization of transmitted data needs to be conducted in forward and backward transmissions. Several quantization methods have been investigated in the literature, which may or may not preserve the initial average [20]–[22].

In this paper, we adopt the probabilistic/dithered quantization methods proposed in [23]–[26]. Denote the quantization operator as $\mathcal{Q}(\mathbf{d})$ for vector $\mathbf{d}$. The ith entry of $\mathcal{Q}(\mathbf{d})$ is calculated as follows [20], [26]:

$$\mathcal{Q}_i(\mathbf{d}) = \lfloor d_i + r[0,\Delta] \rfloor \tag{2}$$

where $r[0,\Delta]$ is a uniform random variable with the limits of $[0,\Delta]$, Δ is the resolution of the quantized channel, and $\lfloor\ \rfloor$ is the floor operation. We can then write the dynamics of the network with quantization at each time step k as

$$\mathbf{v}_q[k] = \mathcal{Q}(\mathbf{v}[k]) = \mathcal{Q}(K_2 H \mathbf{s}_q[k]) \tag{3}$$

$$\begin{aligned} \mathbf{s}_q[k+1] &= \mathcal{Q}(\mathbf{s}[k+1]) = \mathcal{Q}(K_1 H^T \mathbf{v}_q[k]) \\ &= \mathcal{Q}(K_1 H^T \mathcal{Q}(K_2 H \mathbf{s}_q[k])) \end{aligned} \tag{4}$$

where $\mathbf{s}[k] \in \mathcal{R}^{n\times 1}$ and $\mathbf{s}_q[k] \in \mathcal{R}^{n\times 1}$ are the sensor values prior to and after quantization, respectively, and $\mathbf{v}[k] \in \mathcal{R}^{m\times 1}$ and $\mathbf{v}_q[k]$ are VFC values prior to and after quantization, respectively. The initial quantized sensor values are $\mathbf{s}_q[1]$ within the quantization range $[-U, U]$. Define the maximum and minimum of quantized sensor values at time step k as $\max_i \mathbf{s}_{q_i}[k]$

and $\min_i \mathrm{s}_{q_i}[k]$. Here, U satisfies $U \geq |\max_i(\mathrm{s}_{q_i}[1])| + |\min_i(\mathrm{s}_{q_i}[1])|$.

As noted in [23], the above "dithered quantization" is equivalent to the following "probabilistic quantization" method:

$$\mathcal{Q}_i(\mathrm{d}) = \begin{cases} \lfloor d_i \rfloor, & \text{with probability } \frac{\lceil d_i \rceil - d_i}{\Delta} \\ \lceil d_i \rceil, & \text{with probability } 1 - \frac{\lceil d_i \rceil - d_i}{\Delta} \end{cases} \tag{5}$$

where $\lceil\ \rceil$ is the ceiling operator.

E. Network Dynamics With the Employment of Additional Local Memories

Driven by the motivation to further reduce transmitted data, we pursue the employment of additional memories at local sensors. As sensor values are increasingly correlated across time, less valuable information needs to be transmitted. We can, therefore, use additional memories at local sensors and VFCs to hold data in common, and only transmit the informative value difference to reduce the volume of transmitted data. With that consideration in mind, the consensus protocol with the employment of additional local memories is summarized in the following two steps:

Step 1 (Initiation, $k = 1$):

1) Sensor nodes send their quantized values of initial sensor values $\mathrm{s}_m[1]$, denoted as $\mathrm{s}_t[1]$, to their connected VFCs.
2) All VFCs compute the averages, store them in $\mathrm{v}_m[1]$, and send the quantized values $\mathrm{v}_t[1]$ to the connected sensor nodes.
3) All sensor nodes compute the averages of values sent from VFCs, and store copies in their memories $\mathrm{s}_m[2]$.

Step 2 (Iteration, $k > 1$):

1) All sensor nodes compute the quantized difference of local memory values stored in $\mathcal{Q}(\mathrm{s}_m[k])$, denoted as $\mathrm{s}_t[k] \in \mathcal{R}^{n\times 1}$, to be transmitted to the connected VFCs.
2) All VFCs calculate the averages received from the sensor nodes and add them to the local VFC memories, denoted as $\mathrm{v}_m[k]$.
3) All VFCs compute the quantized difference of memory values stored in $\mathrm{v}_m[k]$, and send the quantized averages $\mathrm{v}_t[k] \in \mathcal{R}^{m\times 1}$ to the sensor nodes.
4) All sensor nodes calculate the averages, and add them to their local memories to form $\mathrm{s}_m[k+1]$.

Network dynamics using the above consensus protocol are captured by the following mathematical equations:

$$\begin{cases} \mathrm{s}_t[1] = \mathcal{Q}(\mathrm{s}_m[1]) \\ \mathrm{v}_m[1] = K_2 H \mathrm{s}_t[1] \\ \mathrm{v}_t[1] = \mathcal{Q}(\mathrm{v}_m[1]) \\ \mathrm{s}_m[2] = K_1 H^T \mathrm{v}_t[1] \end{cases} \tag{6}$$

$$\begin{cases} \mathrm{s}_t[k] = \mathcal{Q}(\mathrm{s}_m[k]) - \mathcal{Q}(\mathrm{s}_m[k-1])) \\ \mathrm{v}_m[k] = K_2 H \mathrm{s}_t[k] + \mathrm{v}_m[k-1] \\ \mathrm{v}_t[k] = \mathcal{Q}(\mathrm{v}_m[k]) - \mathcal{Q}(\mathrm{v}_m[k-1]) \\ \mathrm{s}_m[k+1] = K_1 H^T \mathrm{v}_t[k] + \mathrm{s}_m[k]. \end{cases} \tag{7}$$

As shown in (7), the error terms $\mathcal{Q}(\mathrm{s}_m[k] - \mathrm{s}_m[k-1])$, instead of original quantized sensor values, are transmitted. As the information content of error is smaller than that of the original sensor value, a smaller data volume needs to be transmitted, by using fewer bits to code the data. We notice that other ways of adding local memories may not always lead to convergence. The local memories at VFCs are important to guarantee the converging behavior.

III. Asymptotic and Transient Performance of Probabilistic Quantized Consensus in MLMG Networks

In this section, we explore asymptotic and transient properties of quantized consensus in MLMG networks with limited transmission rates. Quantization introduces nonlinearity to distributed consensus and adds to the complexity of analysis. We here provide a brief review of the quantized consensus literature, so as to motivate and delineate our work.

A. Literature Review

A burst of literature on quantized consensus in egalitarian distributed networks has emerged in the past few years. In [15] and [16], the quantization effect is coarsely modeled as an additive noise. Using this quantization model, along with detailed communication and coding models, the authors show that the variance of quantization noise varnishes with time, leading to the convergence of consensus in the mean squared sense. In [17], both the state and the transmitted values are quantized. Lyapunov-type analysis is carried out to prove convergence. As the initial average is not preserved using this quantization scheme, drifting of the converged consensus is expected. Carli *et al.* studied this problem from a different angle [18]–[20]. They utilized the quantized information in a way to preserve the initial average at each iteration [18]. However, the final consensus values may show discrepancies among themselves. The asymptotic discrepancy is either estimated using the additive noise quantization model or bounded by using worse case scenarios [18], [19]. Additional coding schemes are studied in [20] and [21] to speed up the consensus. Similarly, in [22], [27]–[29], deterministic quantization rules are applied to the gossip consensus algorithm to preserve the initial average at each iteration and Layponov analysis is carried out to bound the expected consensus time.

Probabilistic and dithered quantization as described in (2) and (5) (see also [23]–[26]) were developed to remove the asymptotic discrepancies among agents as observed in [18]–[20]. Besides the asymptotic convergence with probability 1, several additional features of the method include.

1) The mean of the converged values is equal to the original average.
2) The variance of the converged values can be made arbitrarily small.
3) Convergence rate characteristics have been characterized.

The use of probabilistic quantization in gossip consensus algorithms for egalitarian networks can also be found in [30] and [31]. All these existing works on probabilistic and dithered quantization are concerned with pure average consensus in egalitarian distributed networks, which has a feature that plays an

important role in the analysis: the system matrix is doubly stochastic. Our system matrix for MLMG networks, A, is not doubly stochastic. We here extend the analysis to MLMG structures, which violate the double stochasticity properties. Of relevance, some efforts have been devoted to weighted averaging in the absence of double stochasticity, for different quantization mechanisms [32], [33].

B. Preliminaries

Lemma 1 ([10]): The necessary and sufficient condition for an MLMG network with standard dynamics (1) to reach consensus is that a path between any pair of sensor nodes exists in the MLMG network. The final consensus value can be expressed in terms of the MLMG topology matrix H, as a weighted sum of the initials $\frac{1}{\mathbf{1}_{1\times m}H\mathbf{1}_{n\times 1}}\mathbf{1}_{1\times m}H\mathbf{x}[1]$.

These results were obtained through analyzing dynamics of the equivalent egalitarian distributed structures captured by the system matrix A. We show that the largest eigenvalue of A is 1, and all other eigenvalues are real, simple, and residing in $[0, 1)$. The second largest eigenvalue, related to consensus time, can also be expressed in terms of H as indicated by the following lemma.

Lemma 2 ([10]): Consider a regular 2LMG. The second largest eigenvalue, λ_2, of the system matrix A can be represented as the maximum of $\frac{1}{r}\sum_{i=1}^{m}(Hy)_i^2$, where r is the regular degree of VFCs, and y is subject to the following constraints: 1) $\sum_{i=1}^{n}K_{1i}^{-1}y_i = 0$; and 2) $\sum_{i=1}^{n}K_{1i}^{-1}y_i^2 = 0$.

Lemma 2 provides an algebraic approach to calculating the second largest eigenvalue directly from the MLMG topology matrix H.

C. Asymptotic Properties

Using the probabilistic quantization method (5), we show in this section that probabilistic quantized consensus can be reached in MLMG networks asymptotically with probability 1. We note that the final consensus value may be different in deferent sample runs. In the next theorem, we calculate the expectation of the final consensus value.

Theorem 1: Consider the probabilistic quantized consensus dynamics shown in (3) and (4). If there exists a path between any pair of sensor nodes, consensus in the presence of quantization can be reached with probability 1. More specifically, there exists a constant c for each sample run such that

$$P\left(\lim_{k\to\infty}\mathbf{s}[k] = c\mathbf{1}_{n\times 1}\right) = 1. \tag{8}$$

Proof: We construct a Markov chain to track the quantized values of the sensor states, denoted as $\mathbf{s}_q[k]$. The states of the finite-state Markov chain belong to the combinations of all possible quantized values between the minimum and maximum of the initials $[-U, U]$. The transition probability $P(\mathbf{s}_q[k+1]|\mathbf{s}_q[k])$ is determined by the dynamics shown in (3) and (4). To prove that consensus at $c\mathbf{1}_{n\times 1}$ can be reached with probability 1, we first show that $c\mathbf{1}_{n\times 1}$ are recurrent states, and then show that all other states are transient states, which can reach at least one of the recurrent states with a positive probability.

It is straightforward to show that $c\mathbf{1}_{n\times 1}$ are recurrent states for each particular constant c. As K_2H and K_1H^T are both stochastic matrices with row sums being 1, when $\mathbf{s}_q[k]$ reach $c\mathbf{1}_{n\times 1}$, we will have $\mathbf{s}_q[k+1] = \mathbf{s}_q[k]$.

Now let us show that all states that are not in the form of $c\mathbf{1}_{n\times 1}$ are transient states, which can reach at least one of the recurrent states with a positive probability. It suffices to show that there exists a recurrent state such that the Markov chain starting from any $\mathbf{s}_q[0] \neq c\mathbf{1}_{n\times 1}$ can reach it with a positive probability. We choose $\lfloor\hat{c}\rfloor\,\mathbf{1}_{n\times 1}$ to be this particular state, where $\hat{c} = \frac{1}{\mathbf{1}_{1\times m}H\mathbf{1}_{n\times 1}}\mathbf{1}_{1\times m}H\mathbf{s}_q[0]$. To show this, we first prove that there exists a positive probability that

$$\begin{aligned}&||\mathbf{s}_q[k+1] - \hat{c}\mathbf{1}_{n\times 1}||_\infty \\ &\quad= ||\mathcal{Q}[K_1H^T\mathcal{Q}(K_2H\mathbf{s}_q[k])] - \hat{c}\mathbf{1}_{n\times 1}||_\infty \\ &\quad< ||\mathbf{s}_q[k] - \hat{c}\mathbf{1}_{n\times 1}||_\infty \end{aligned}\tag{9}$$

for every k until all elements of $\mathbf{s}[k]$ reach the neighboring quantized values of $\hat{c}$, $\lfloor\hat{c}\rfloor$, or $\lceil\hat{c}\rceil$. We then show that at the next time instance, $\lfloor\hat{c}\rfloor\,\mathbf{1}_{n\times 1}$ can be reached with some positive probability. The second step is straightforward due to the property of probabilistic quantization.

To prove (9), we define a specific path in the Markov chain to reach the neighboring quantized values of $\hat{c}$. In particular, in the two probabilistic quantization operations "$\mathcal{Q}()$" in (9), we assign each entry with a quantized value nearest to $\hat{c}$ if the entry is above $\lceil\hat{c}\rceil$ or below $\lfloor\hat{c}\rfloor$ (which is possible as with a positive probability). If an entry $s_{q_i}[k]$ already reaches $\lfloor\hat{c}\rfloor$ or $\lceil\hat{c}\rceil$ and all possible choices of $\mathbf{s}_q[k+1]$ are in the range of $[\lfloor\hat{c}\rfloor, \lceil\hat{c}\rceil]$, we do not update it.

If an entry $\mathbf{s}_i[k]$ is outside the range of $[\lfloor\hat{c}\rfloor, \lceil\hat{c}\rceil]$, the operations of left multiplying K_2H and K_1H^T (with row sums equaling to 1) and the operation of choosing the quantized value closest to $\hat{c}$ will shorten the maximum distance of all entries to $\hat{c}$, if $\hat{c}$ can be reached without quantization. The infinity norm as shown in (9) is, hence, reduced for each iteration. ■

The final quantized consensus value c can be different for each sample run. We show in the next theorem that the expectation of the final quantized consensus value c for all sample runs is a weighted sum of the initial values, and is equal to the final consensus value without quantization, $\hat{c}$.

Theorem 2: Consider the probabilistic quantized consensus shown in (3) and (4). If there exists a path between any pair of sensor nodes, the expectation of the final quantized consensus value equals $\hat{c}$ for the initial condition $\mathbf{s}_q[1]$.

Proof: We rewrite the dithered quantized dynamics (3) and (4) as

$$\mathbf{v}_q[k] = \mathcal{Q}(K_2H\mathbf{s}_q[k]) = K_2H\mathbf{s}_q[k] + \mathbf{u}_1[k] \tag{10}$$

$$\begin{aligned}\mathbf{s}_q[k+1] &= \mathcal{Q}(K_1H^T\mathbf{v}_q[k]) \\ &= K_1H^T\mathbf{v}_q[k] + \mathbf{u}_2[k] \\ &= K_1H^TK_2H\mathbf{s}_q[k] + K_1H^T\mathbf{u}_1[k] + \mathbf{u}_2[k]\end{aligned}\tag{11}$$

where the vectors $\mathbf{u}_1[k] \in R^m$ and $\mathbf{u}_2[k] \in R^n$ are additive noises. Taking expectation of the above equation, we obtain

$$E(\mathbf{s}_q[k+1]) = K_1 H^T K_2 H E(\mathbf{s}_q[k]) + K_1 H^T E(\mathbf{u}_1[k]) + E(\mathbf{u}_2[k])). \quad (12)$$

We note that the theorem is proved if $E(\mathbf{u}_1[k]) = \mathbf{0}$ and $E(\mathbf{u}_2[k]) = \mathbf{0}$, as the recursion of $E(\mathbf{s}_q[k])$ is precisely the same as that of $\mathbf{x}[k]$ without quantization for the initial condition $\mathbf{x}[1] = \mathbf{s}[1] = \mathbf{s}_q[1]$. In order to show that $E(\mathbf{u}_1[k]) = \mathbf{0}$ and $E(\mathbf{u}_2[k]) = \mathbf{0}$, we only need to show that the expectation of each entry in the additive noise vectors is 0. This can be done in a straightforward way using $\mathbf{u}_1[k]$ as an example. According to the probabilistic quantization rules specified in (5)

$$E(u_{1i}[k]) = (\lceil z_{1i} \rceil - z_{1i}) \frac{z_{1i} - \lfloor z_{1i} \rfloor}{\Delta} + (\lfloor z_{1i} \rfloor - z_{1i}) \frac{\lceil z_{1i} \rceil - z_{1i}}{\Delta} = 0 \quad (13)$$

where z_{1i} is the ith entry of $K_2 H \mathbf{s}_q[k]$. ■

D. Transient Properties

In this section, we study the consensus time of the quantized consensus algorithm in MLMG networks. In the first result, we bound the difference between the expected transient dynamics and the expected final consensus value using the second largest eigenvalue. The second result is concerned with bonding the expected range of quantized transient dynamics.

Theorem 3: Consider the probabilistic quantized consensus [shown in (3) and (4)]. If there exists a path between any pair of sensor nodes, the following bounds for the transient expectation of the quantized sensor values hold for $k \geq 2$

$$||K_1^{-\frac{1}{2}}(E(\mathbf{s}_q[k]) - \hat{c}\mathbf{1})|| \leq \lambda_2^{k-1} ||K_1^{-\frac{1}{2}}(E(\mathbf{s}_q[1]) - \hat{c}\mathbf{1})|| \quad (14)$$

$$||E(\mathbf{s}_q[k]) - \hat{c}\mathbf{1}|| \leq \left(\frac{d_{s_{\max}}}{d_{s_{\min}}}\right)^{\frac{1}{2}} \lambda_2^{k-1} ||E(\mathbf{s}_q[1]) - \hat{c}\mathbf{1}|| \quad (15)$$

where the maximal and minimal degrees of sensor nodes are $d_{s_{\max}}$ and $d_{s_{\min}}$.

Proof: Equation (12) leads to

$$E(\mathbf{s}_q[k]) = K_1 H^T K_2 H E(\mathbf{s}_q[k-1]). \quad (16)$$

Multiplying $K_1^{-\frac{1}{2}}$ to the left of both sides of (16), we obtain

$$K_1^{-\frac{1}{2}} E(\mathbf{s}_q[k]) = K_1^{-\frac{1}{2}} A K_1^{\frac{1}{2}} K_1^{-\frac{1}{2}} E(\mathbf{s}_q[k-1]) = K_1^{\frac{1}{2}} H^T K_2 H K_1^{\frac{1}{2}} (K_1^{-\frac{1}{2}} E(\mathbf{s}_q[k-1])). \quad (17)$$

The new system matrix $\hat{A} = K_1^{\frac{1}{2}} H^T K_2 H K_1^{\frac{1}{2}}$ is symmetric, and shares a common set of eigenvalues with $K_1 H^T K_2 H$ [10].

Now let us calculate $||(K_1^{-\frac{1}{2}}(E(\mathbf{s}_q[k]) - \hat{c}\mathbf{1})||$ as follows:

$$\begin{aligned} &||K_1^{-\frac{1}{2}}(E(\mathbf{s}_q[k]) - \hat{c}\mathbf{1})|| \\ &= ||\hat{A}(K_1^{-\frac{1}{2}} E(\mathbf{s}_q[k-1])) - K_1^{-\frac{1}{2}} \hat{c}\mathbf{1})|| \\ &= ||(\hat{A} - \hat{A}^\infty)(K_1^{-\frac{1}{2}} E(\mathbf{s}_q[k-1]) - K_1^{-\frac{1}{2}} \hat{c}\mathbf{1})|| \\ &\leq ||\hat{A} - \hat{A}^\infty||^{k-1} ||K_1^{-\frac{1}{2}}(E(\mathbf{s}_q[1]) - \hat{c}\mathbf{1})||. \end{aligned} \quad (18)$$

The matrix $\hat{A} - \hat{A}^\infty$ is symmetric, and as such $||\hat{A} - \hat{A}^\infty||$ equals the largest eigenvalue of $\hat{A} - \hat{A}^\infty$ and $A - A^\infty$. It also equals λ_2 of $K_1 H^T K_2 H$ using eigenvalue decomposition. Clearly, (14) is satisfied. Note that $K_1^{-\frac{1}{2}}$ is a diagonal matrix of the square roots of degrees for all sensors, we have

$$||K_1^{-\frac{1}{2}}(E(\mathbf{s}_q[k]) - \hat{c}\mathbf{1})|| \leq d_{s_{\max}}^{\frac{1}{2}} ||E(\mathbf{s}_q[k]) - \hat{c}\mathbf{1})|| \quad (19)$$

$$||K_1^{-\frac{1}{2}}(E(\mathbf{s}_q[k]) - \hat{c}\mathbf{1})|| \geq d_{s_{\min}}^{\frac{1}{2}} ||E(\mathbf{s}_q[k]) - \hat{c}\mathbf{1})||. \quad (20)$$

Equations (14)–(20) lead to (15) with simple algebra. ■

Equation (15) naturally leads to the following corollary on the expected consensus time (for the norm-2 difference between the expected sensor values and the expected final consensus value to fall within δ of the initials). Of note, we do not limit ourselves to a small δ here, and as such the result holds for any quantization resolution of interest.

Corollary 1: The expected consensus time for the probabilistic quantized consensus [shown in (3) and (4)] is upper bounded by $\log_{\lambda_2}(\delta(\frac{d_{s_{\min}}}{d_{s_{\max}}})^{\frac{1}{2}})$.

Define the range of quantized sensor values as $\overline{\mathbf{s}_q}[k]$. Clearly, $\max_i \mathbf{s}_{q_i}[k] \leq \max_i \mathbf{s}_{q_i}[k-1]$, $\min_i \mathbf{s}_{q_i}[k] \geq \min_i \mathbf{s}_{q_i}[k-1]$, and $\overline{\mathbf{s}_q}[k] \leq \overline{\mathbf{s}_q}[k-1]$ by a convex hull type of argument [23]. The expected range of quantized sensor values, denoted as $E(\overline{\mathbf{s}_q}[k])$, can be bounded as shown in the following theorem.

Theorem 4: Consider the probabilistic quantized consensus [shown in (3) and (4)]. If there exists a path between any pair of sensor nodes, the following bounds for the expected range of quantized sensor values hold for $k \geq 2$

$$E(\overline{\mathbf{s}_q}[k]) \leq 2\left(\frac{d_{s_{\max}}}{d_{s_{\min}}}\right)^{\frac{1}{2}} \lambda_2^{k-1} ||\mathbf{s}_q[1] - \hat{c}\mathbf{1}|| + \left(\frac{d_{s_{\max}}}{d_{s_{\min}}}\right)^{\frac{1}{2}} \frac{1 - \lambda_2^{k-2}}{1 - \lambda_2} (||K_1 H^T|| \sqrt{n} + \sqrt{m})\Delta. \quad (21)$$

As $k \to \infty$, we have

$$\lim_{k\to\infty} E(\overline{\mathbf{s}_q}[k]) \leq \left(\frac{d_{s_{\max}}}{d_{s_{\min}}}\right)^{\frac{1}{2}} \frac{(||K_1 H^T|| \sqrt{n} + \sqrt{m})\Delta}{1 - \lambda_2}. \quad (22)$$

Proof:

$$E(\overline{\mathbf{s}_q}[k]) = E(\max_i \mathbf{s}_{q_i}[k] - \min_i \mathbf{s}_{q_i}[k]). \quad (23)$$

Now consider $E(\max_i \mathrm{s}_{q_i}[k])$. According to the ordered statistics for a sequence of random variables [23], [34], we have

$$E(\max_i \mathrm{s}_{q_i}[k]|\mathrm{s}_{q_i}[k-1]) \le \max_i (E(\mathrm{s}_{q_i}[k]|\mathrm{s}_{q_i}[k-1])) + E(\max_i(\mathrm{s}_{q_i}[k] - E(\mathrm{s}_{q_i}[k]))|\mathrm{s}_{q_i}[k-1]). \quad (24)$$

According to (11), we have

$$\max_i E(\mathrm{s}_{q_i}[k]|\mathrm{s}_{q_i}[k-1]) = \max_i(K_1 H^T K_2 H \mathrm{s}_q[k-1]) \quad (25)$$

$$\begin{aligned} &E(\max_i(\mathrm{s}_{q_i}[k] - E(\mathrm{s}_{q_i}[k]))|\mathrm{s}_q[k-1]) \\ &= E(\max_i(K_1 H^T K_2 H \mathrm{s}_q[k-1] + K_1 H^T \mathbf{u}_1[k-1] \\ &\quad + \mathbf{u}_2[k-1] - K_1 H^T K_2 H E(\mathrm{s}_q[k-1]))|\mathrm{s}_q[k-1]) \\ &= E(\max_i(K_1 H^T \mathbf{u}_1[k-1] + \mathbf{u}_2[k-1])|\mathrm{s}_q[k-1]). \end{aligned} \quad (26)$$

Combining 24–26, and taking exception with respect to $\mathrm{s}_q[k-1]$, we obtain

$$E(\max_i \mathrm{s}_{q_i}[k]) \le E(\max_i(A\mathrm{s}_q[k-1])) + E(\max_i(K_1 H^T \mathbf{u}_1[k-1] + \mathbf{u}_2[k-1])). \quad (27)$$

Similarly, we have the following results for $E(\min_i \mathrm{s}_{q_i}[k])$:

$$E(\min_i \mathrm{s}_{q_i}[k]) \ge E(\min_i(A\mathrm{s}_q[k-1])) - E(\max_i(K_1 H^T \mathbf{u}_1[k-1] + \mathbf{u}_2[k-1])). \quad (28)$$

Equations (27) and (28) lead to

$$E(\overline{\mathrm{s}_q}[k]) \le E(\max_i(A\mathrm{s}_q[k-1]) - \min_i(A\mathrm{s}_q[k-1])) + 2E(\max_i(K_1 H^T \mathbf{u}_1[k-1] + \mathbf{u}_2[k-1])). \quad (29)$$

Recursively applying (29) through expressing $\mathrm{s}_q[k-1]$ in terms of $\mathrm{s}_q[k-2], \ldots, \mathrm{s}_q[1]$, we obtain

$$\begin{aligned} E(\overline{\mathrm{s}_q}[k]) &\le \max_i(A^{k-1}\mathrm{s}_q[1]) - \min_i(A^{k-1}\mathrm{s}_q[1]) \\ &\quad + 2\sum_{i=1}^{k-1} E(\max_i(A^{k-i-1}(K_1 H^T \mathbf{u}_1[i] + \mathbf{u}_2[i]))) \\ &\le 2\left(\frac{d_{s_{\max}}}{d_{s_{\min}}}\right)^{\frac{1}{2}} \lambda_2^{k-1}||\mathrm{s}_q[1] - \hat{c}\mathbf{1}|| \\ &\quad + 2\sum_{i=1}^{k-1}\left(\frac{d_{s_{\max}}}{d_{s_{\min}}}\right)^{\frac{1}{2}} \lambda_2^{k-i-1} E(||K_1 H^T \mathbf{u}_1[i] + \mathbf{u}_2[i]||). \end{aligned} \quad (30)$$

Now consider to bound the second part of (30)

$$E(||K_1 H^T \mathbf{u}_1[i] + \mathbf{u}_2[i]||) \le ||K_1 H^T||E(||\mathbf{u}_1[i]||) + E(||\mathbf{u}_2[i]||). \quad (31)$$

According to Jensen's inequality and (13), we have

$$\begin{aligned} E(||\mathbf{u}_2[i]||) &\le \left(\sum_j E(u_{2j}[i])^2\right)^{\frac{1}{2}} \\ &= \left(\sum_j \left((\lceil z_{2j}\rceil - z_{2j})^2 \frac{z_{2j} - \lfloor z_{2j}\rfloor}{\Delta} + (\lfloor z_{2j}\rfloor - z_{2j})^2 \times \frac{\lceil z_{2j}\rceil - z_{2j}}{\Delta}\right)\right)^{\frac{1}{2}} \le \left(n\frac{\Delta^2}{4}\right)^{\frac{1}{2}} = \frac{\sqrt{n}\Delta}{2} \end{aligned} \quad (32)$$

where z_{2j} is the jth entry of $K_1 H^T \mathbf{v}_q[k]$. The calculation of $E(||\mathbf{u}_1[i]||)$ is similar. In all, we can bound $E(\overline{\mathrm{s}_q}[k])$ as

$$E(\overline{\mathrm{s}_q}[k]) \le 2\left(\frac{d_{s_{\max}}}{d_{s_{\min}}}\right)^{\frac{1}{2}} \lambda_2^{k-1}||\mathrm{s}_q[1] - \hat{c}\mathbf{1}|| + \left(\frac{d_{s_{\max}}}{d_{s_{\min}}}\right)^{\frac{1}{2}} \frac{1-\lambda_2^{k-2}}{1-\lambda_2}(||K_1 H^T||\sqrt{n} + \sqrt{m})\Delta. \quad (33)$$

The rest of the results follow naturally. ■

A similar argument leads to the following corollary. The proof is omitted due to the limited space.

Corollary 2: Consider the probabilistic quantized consensus [shown in (3) and (4)]. If there exists a path between any pair of sensor nodes, the following bound for the expected norm hold:

$$E(||\mathrm{s}_q[k] - \hat{c}\mathbf{1}||) \le \left(\frac{d_{s_{\max}}}{d_{s_{\min}}}\right)^{\frac{1}{2}} \lambda_2^{k-1}||\mathrm{s}_q[1] - \hat{c}\mathbf{1}|| + \left(\frac{d_{s_{\max}}}{d_{s_{\min}}}\right)^{\frac{1}{2}} \frac{1-\lambda_2^{k-2}}{1-\lambda_2}\frac{(||K_1 H^T||\sqrt{n} + \sqrt{m})\Delta}{2}. \quad (34)$$

IV. Explicit Structural Interpretation on the Number of Transmissions to Reach Consensus

In this section, we take a structural approach to exploring advantages of the MLMG structures over traditional egalitarian distributed structures. For broad classes of MLMG structures, we provide explicit mathematical expressions for the number of transmissions needed to reach consensus based on simple characteristics of MLMG structures (such as the regular degrees and numbers of sensors and VFCs). We also calculate the reduced number of transmissions compared to their equivalent egalitarian distributed networks. Here we denote $N(\,)$ and $t(\,)$ as the number of transmission per iteration and the expected consensus time bound of for the structure in $(\,)$. Clearly, $t(\mathcal{G}) = t(\tilde{\mathcal{G}})$ due to the equivalence of dynamics between this two structures, which can be seen from (1) and (12).

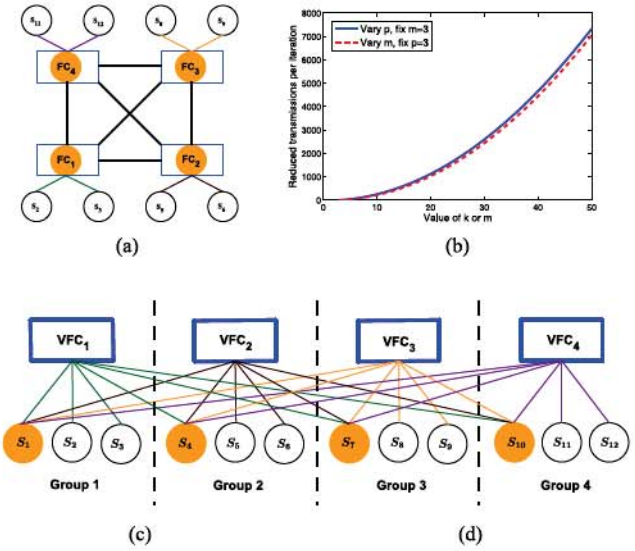

Fig. 2. MLMG structure with a complete graph among the group leaders. (a) FC version. (b) VFC version. (c) Number of reduced transmissions per iteration grows quadratically with the network size.

A. Complete Graph Among Group Leaders

We consider a broad class of MLMG structures with the communications among group leaders forming a complete graph. This structure can be useful when the VFCs are within a short communication range, and hence, are naturally connected in a complete graph fashion, or when the number of VFCs is small, and hence, establishing a complete topology among the VFCs is not transmission-expensive. In particular, the network is composed of m groups, each with a group leader (FC or VFC). In the FC version, each group has p sensor nodes, including the leader sensor node, which can merge to the FC. Each FC communicates with all other FCs in the network. In the equivalent VFC version, each VFC communicates to all sensor nodes within its group and all leader sensor nodes in the other groups. Nonleader sensor nodes only communicate with the VFC within their groups. No other communication exists. An example with $m = 4$ and $p = 3$ is shown in Fig. 2(a) and (c). We analyze the number of transmissions that can be saved for this class of MLMG structures. Before presenting the theorem, we first recall from [10] a lemma, which explicitly expresses λ_2 in terms of simple structural characteristics of H.

Lemma 3 ([10]): Consider the MLMG structure $\mathcal{G}_{\text{comp}}$ ($m > 1$ and $p > 1$) with a complete graph among the FCs described above. The second largest eigenvalue λ_2 for $\mathcal{G}_{\text{comp}}$ is $\frac{p-1}{p+m-1}$.

Lemma 3 relates simple structural characteristics (m and p) to λ_2, and, hence, the consensus time $t(\mathcal{G}_{\text{comp}})$. For instance, using the expected consensus time expression shown in Theorem 3 and Corollary 1, $t(\mathcal{G}_{\text{comp}}) = \log_{\frac{p-1}{p+m-1}}(\delta(\frac{d_{s\min}}{d_{s\max}})^{\frac{1}{2}})$. We note that a similar consensus time measure can be obtained based on the transient bound expressed in Theorem 4. The following theorem expresses the number of transmissions to reach consensus in terms of $t(\mathcal{G}_{\text{comp}})$, which is a function of simple structural characteristics.

Theorem 5: Consider the probabilistic quantized consensus [shown in (3) and (4)] defined on the MLMG structure $\mathcal{G}_{\text{comp}}$ and its equivalent distributed egalitarian structure $\tilde{\mathcal{G}}_{\text{comp}}$ of the same dynamics, defined on the system matrix A. The number of transmissions to reach consensus per iteration in the $\mathcal{G}_{\text{comp}}$ structure is $N(\mathcal{G}_{\text{comp}}) = 2(p + m - 1)m$, and that in the $\tilde{\mathcal{G}}_{\text{comp}}$ structure is $N(\tilde{\mathcal{G}}_{\text{comp}}) = [m(pm - 1) + (p - 1)m(p + m - 2)]$. $N(\mathcal{G}_{\text{comp}}) < N(\tilde{\mathcal{G}}_{\text{comp}})$, when $p > 2$ or $m > 2$. In addition, the reduced number of transmissions per iteration grows in an order of $\mathcal{O}(p^2)$ with the increase of p, and in an order of $\mathcal{O}(m^2)$ with the increase of m.

Proof: We first calculate the number of transmissions per iteration in each topology. In the $\mathcal{G}_{\text{comp}}$ structure, as each VFC connects to p sensor nodes within its group and one leader node in each of the other $m - 1$ groups, $p + m - 1$ connections per VFC are expected. Considering the forward and backward transmissions and the consensus time according to Lemma 3, we obtain $N(\mathcal{G}_{\text{comp}}) = 2(p + m - 1)mt(\mathcal{G}_{\text{comp}})$. In the $\tilde{\mathcal{G}}_{\text{comp}}$ structure, as each of the m leader nodes through the VFCs connects to all other $pm - 1$ sensor nodes, a total of $p(pm - 1)$ transmissions are needed for these leader nodes. In addition, as each of the $p - 1$ sensor nodes in each of the m groups communicates to $p - 1$ nodes in its group and all leader nodes in the other $m - 1$ groups, a total of $(p - 1)m(p + m - 2)$ transmissions are needed for these sensor nodes. As the consensus time for both structures are the same according to (1), Lemma 3 leads to $N(\tilde{\mathcal{G}}_{\text{comp}}) = (m(pm - 1) + (p - 1)m(p + m - 2))t(\mathcal{G}_{\text{comp}})$.

Now let us compare $N(\mathcal{G}_{\text{comp}})$ and $N(\tilde{\mathcal{G}}_{\text{comp}})$ per iteration. Simple algebra leads to $N(\tilde{\mathcal{G}}_{\text{comp}}) - N(\mathcal{G}_{\text{comp}}) = m(pm - p - m - 1) + (p + m - 2)(p - 2)m$ per iteration. Clearly, when $p > 2$ and $m \geq 2$ or $p \geq 2$ and $m > 2$, both terms in the above expression are larger than 0. Furthermore, simple observation suggests that the difference in $N(\tilde{\mathcal{G}}_{\text{comp}})$ and $N(\mathcal{G}_{\text{comp}})$ grows in the order of $\mathcal{O}(p^2)$ and $\mathcal{O}(m^2)$. ■

The above theorem suggests the advantage of the MLMG structures in reducing the number of transmissions for large-scale networks. For the example shown in Fig. 2(a), we plot $N(\tilde{\mathcal{G}}_{\text{comp}}) - N(\mathcal{G}_{\text{comp}})$ per iteration versus p and m [see Fig. 2(b)]. The total number of iterations to reach consensus is $N(\mathcal{G}_{\text{comp}})t(\mathcal{G}_{\text{comp}})$ for structure $\mathcal{G}_{\text{comp}}$ and $N(\tilde{\mathcal{G}}_{\text{comp}})t(\tilde{\mathcal{G}}_{\text{comp}})$ for structure $\tilde{\mathcal{G}}_{\text{comp}}$. As the consensus time also increases with the network size, the transmission savings can be significant for large-scale networks. One further note is that we include the transmissions between the leader nodes and the VFCs in our calculation, which, if ignored in a realistic setting, further reduces the number of transmissions.

The theorem also suggests that the total transmission load can be expressed in terms of simple MLMG structure characteristics (such as the degrees and numbers of sensors and VFCs). Such explicit structural results enable an optimal design of MLMG structures (with a complexity of $\mathcal{O}(1)$) to meet performance requirements. No complicated numerical optimization is needed, thus, making the network design procedures *scalable* to large-scale networks. We note that here we characterize consensus properties directly using the MLMG topology matrix H, instead of the system matrix A on which traditional egalitarian

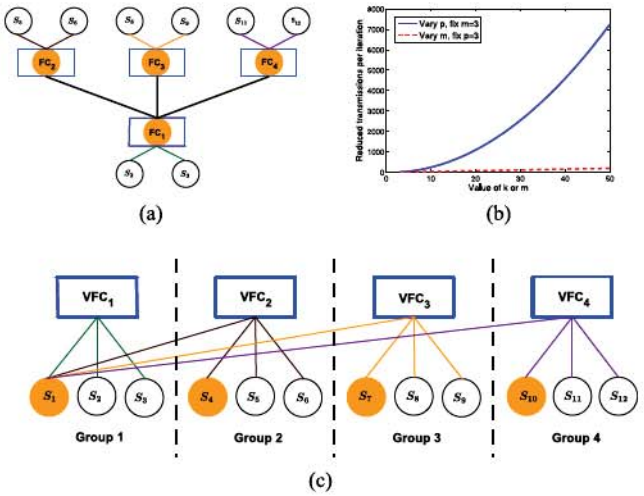

Fig. 3. MLMG structure with a centralized graph among the leaders. (a) FC version. (b) VFC version. (c) Number of reduced transmissions per iteration grows quadratically with the network size.

network control has been focused. The MLMG topology matrix H exposes hidden structures that are not observable in A, and provides us with new insightful structural perspectives to the analysis of consensus performance.

B. Centralized Graph Among the Leaders

Now consider a broad class of MLMG structures with a centralized communication graph among the group leaders. In particular, the network is composed of m groups, each with an FC. Each group has p sensor nodes, including the leader sensor node. The leader sensor node in one and only one group communicates with all VFCs in the network. All other sensor nodes in each group only communicate with the VFC within the group. No other communication exists. An example with $m = 4$ and $p = 3$ is shown in Fig. 3(a) and (c). FC_1 of group 1 communicates with all other group leaders.

Lemma 4 ([10]): Consider the MLMG structure $\mathcal{G}_{\text{cen}}$ ($m > 2$ and $p > 1$) with a centralized graph among the FCs described above. The second largest eigenvalue λ_2 for $\mathcal{G}_{\text{cen}}$ is $\frac{p}{p+1}$.

According to Lemma 4, we can express consensus time, $t(\mathcal{G}_{\text{cen}})$ in terms of a simple structural characteristic p. For instance, using the expected consensus time expression shown in Theorem 3 and Corollary 1, we have $t(\mathcal{G}_{\text{cen}}) = \log_{\frac{p}{p+1}}(\delta(\frac{d_{s\min}}{d_{s\max}})^{\frac{1}{2}})$. A similar result can be obtained based on the consensus time measure expressed in Theorem 4.

Theorem 6: Consider the probabilistic quantized consensus [shown in (3) and (4)] defined on the MLMG structure $\mathcal{G}_{\text{cen}}$ and its equivalent distributed egalitarian structure $\tilde{\mathcal{G}}_{\text{cen}}$. The number of transmissions to reach consensus per iteration in the $\mathcal{G}_{\text{cen}}$ structure is $N(\mathcal{G}_{\text{cen}}) = 2(pm + m - 1)$, and that in the $\tilde{\mathcal{G}}_{\text{cen}}$ structure is $N(\tilde{\mathcal{G}}_{\text{cen}}) = pm - 1 + (p-1)^2 + p^2(m-1)$. $N(\mathcal{G}_{\text{cen}}) < N(\tilde{\mathcal{G}}_{\text{cen}})$, when $p > 2$ and $m > 2$. In addition, the reduced number of transmissions per iteration grows in an order of $\mathcal{O}(p^2)$ with the increase of p, and in an order of $\mathcal{O}(m)$ with the increase of m.

The proof is very similar to the proof of Theorem 5, and thus, the details are omitted. The total number of iterations to reach consensus is $N(\mathcal{G}_{\text{cen}})t(\mathcal{G}_{\text{cen}})$ for structure $\mathcal{G}_{\text{cen}}$ and $N(\tilde{\mathcal{G}}_{\text{cen}})t(\tilde{\mathcal{G}}_{\text{cen}})$ for structure $\tilde{\mathcal{G}}_{\text{cen}}$.

V. Use of Additional Local Memories to Further Reduce Transmission Load

In this section, we show asymptotic and transient properties of consensus in MLMG networks of digitized channels, with the employment of additional memories at both sensor nodes and VFCs. With growing correlations among sensor values, we can reduce the transmission load by only transmitting differences of sensor values instead of true values. The transmission load that can be further reduced by employing additional memories is also analyzed.

A. Asymptotic and Transient Properties

Theorem 7: Consider the probabilistic quantized consensus dynamics in MLMG networks equipped with memory (6) and (7). If there exists a path between any pair of sensor nodes, consensus can be reached with probability 1. The expectation of the final consensus value equals $\hat{c}$ for initial condition $\mathrm{s}_m[1] = \mathrm{s}_q[1]$. The following bounds for the transient expectation of the quantized sensor values hold

$$\begin{aligned}&||K_1^{-\frac{1}{2}}(E(\mathcal{Q}(\mathrm{s}_m[k])) - \hat{c}\mathbf{1})||\\ &\quad\le \lambda_2^{k-1}||K_1^{-\frac{1}{2}}(E(\mathcal{Q}(\mathrm{s}_m[1])) - \hat{c}\mathbf{1})|| \qquad (35)\\ &||E(\mathcal{Q}(\mathrm{s}_m[k])) - \hat{c}\mathbf{1})||\\ &\quad\le \left(\frac{d_{s\max}}{d_{s\min}}\right)^{\frac{1}{2}}\lambda_2^k||E(\mathcal{Q}(\mathrm{s}_m[1])) - \hat{c}\mathbf{1})||. \qquad (36)\end{aligned}$$

Proof: The comparison between Theorem 7 and Theorems 1 and 2 suggests that it is sufficient to prove that

$$\mathrm{s}_m[k] = \mathrm{s}[k] \qquad (37)$$

$$\mathrm{v}_m[k] = \mathrm{v}[k] \qquad (38)$$

for every k. We use induction for the proof.

When $k = 1$, we have

$$\mathrm{v}_m[1] = K_2 H\mathcal{Q}(\mathrm{s}_m[1]) = K_2 H\mathrm{s}_q[1] = \mathrm{v}[1] \qquad (39)$$

$$\mathrm{s}_m[2] = K_1 H^T\mathcal{Q}(\mathrm{v}_m[1]) = K_1 H^T\mathcal{Q}(\mathrm{v}[1]) = \mathrm{s}[2]. \qquad (40)$$

Suppose for a k, we have $\mathrm{v}_m[k] = \mathrm{v}[k]$ and $\mathrm{s}_m[k+1] = \mathrm{s}[k+1]$. Now let us show that the relationship also holds for $k+1$. To do that, we notice

$$\begin{aligned}\mathrm{v}_m[k+1] &= K_2 H\mathrm{s}_t[k+1] + \mathrm{v}_m[k]\\ &= K_2 H(\mathcal{Q}(\mathrm{s}_m[k+1]) - \mathcal{Q}(\mathrm{s}_m[k])) + \mathrm{v}_m[k]\\ &= K_2 H\mathcal{Q}(\mathrm{s}_m[k+1]) = K_2 H\mathcal{Q}(\mathrm{s}[k+1]) = \mathrm{v}[k+1]\end{aligned} \qquad (41)$$

and similarly

$$\begin{aligned}\mathrm{s}_m[k+2] &= K_1 H^T \mathrm{v}_t[k+1] + \mathrm{s}_m[k+1] \\ &= K_1 H^T (\mathcal{Q}(\mathrm{v}_m[k+1]) - \mathcal{Q}(\mathrm{v}_m[k]) + \mathrm{s}_m[k+1] \\ &= K_1 H^T \mathcal{Q}(\mathrm{v}_m[k+1]) = K_1 H^T \mathcal{Q}(\mathrm{v}[k+1]) = \mathrm{s}[k+2].\end{aligned} \tag{42}$$

■

Theorem 7 naturally leads to the following corollary on the transient performance of $\mathrm{s}_t[k]$.

Corollary 3: Consider the probabilistic quantized consensus dynamics in MLMG networks equipped with memory (6) and (7). If there exists a path between any pair of sensor nodes, consensus can be reached with probability 1. The expectation of the final consensus value equals $\hat{c}$ for initial condition $\mathrm{s}_m[1] = \mathrm{s}_q[1]$. The following bounds for the quantized sensor values sent from sensor nodes hold, where $k > 2$.

$$||K_1^{-\frac{1}{2}} E(\mathrm{s}_t[k])|| \le \lambda_2^{k-2} ||K_1^{-\frac{1}{2}} E(\mathrm{s}_t[2])|| \tag{43}$$

$$||E(\mathrm{s}_t[k])|| \le \left(\frac{d_{s_{\max}}}{d_{s_{\min}}}\right)^{\frac{1}{2}} \lambda_2^{k-2} ||E(\mathrm{s}_t[2])|| \tag{44}$$

$$\begin{aligned}E(\overline{\mathrm{s}_t}[k]) \le\ & 2\left(\frac{d_{s_{\max}}}{d_{s_{\min}}}\right)^{\frac{1}{2}} \lambda_2^{k-2} E(||\mathrm{s}_t[2]||) \\ &+ \left(\frac{d_{s_{\max}}}{d_{s_{\min}}}\right) (||K_1 H^T||\sqrt{n} + \sqrt{m})\Delta\end{aligned} \tag{45}$$

$$\begin{aligned}E(||\mathrm{s}_t[k]||) \le\ & \left(\frac{d_{s_{\max}}}{d_{s_{\min}}}\right)^{\frac{1}{2}} \lambda_2^{k-2} E(||\mathrm{s}_t[2]||) \\ &+ \left(\frac{d_{s_{\max}}}{d_{s_{\min}}}\right) \frac{(||K_1 H^T||\sqrt{n} + \sqrt{m})\Delta}{2}\end{aligned} \tag{46}$$

where $\mathrm{s}_t[2] = \mathrm{s}_m[2] - \mathrm{s}_m[1]$, $||E(s_t[2])|| = ||(I - A)(\mathrm{s}_q[1] - \hat{c}\mathbf{1})||$, and $E(||s_t[2]||) \le ||A - I||||\mathrm{s}_q[1] - \hat{c}\mathbf{1}|| + \frac{(||K_1 H^T||\sqrt{n}+\sqrt{m})\Delta}{2}$.

Proof: According to (7) and (37), we have

$$\begin{aligned}\mathrm{s}_t[k] &= \mathcal{Q}(\mathrm{s}_m[k]) - \mathcal{Q}(\mathrm{s}_m[k-1])) = \mathrm{s}_q[k] - \mathrm{s}_q[k-1] \\ &= (K_1 H^T K_2 H - I)\mathrm{s}_t[k-1].\end{aligned}$$

The rest of the proof is similar to the proofs of Theorems 3 and 4 and, hence, is omitted here. ■

B. Transmission Load Reduction

The layered structure reduces the number of transmissions to reach consensus, and hence, reduces the transmission load to reach consensus. The use of extra memory introduced in Section V-A can further reduce the transmission load, by reducing the number of bits transmitted at each iteration. Different coding schemes, captured by $\mathcal{B}(\mathrm{x})$, can be used. $\mathcal{B}(\mathrm{x})$ is a mapping from a vector with each entry in $[-U, U]$ to the number of bits needed to code entries in the vector. Without loss of generality, we here use $\mathcal{B}(\mathrm{x}) = \lceil \log_2(\frac{|\max_i(\mathrm{x}_i)|+|\min_i(\mathrm{x}_i)|}{\Delta} + 1)\rceil$.

With the knowledge that $\max(\mathrm{v}_q[k]) \le \max(\mathrm{s}_q[k])$ and $\min(\mathrm{v}_q[k]) \ge \min(\mathrm{s}_q[k])$, the expected total number of bits transmitted for an MLMG network $\mathcal{G}$ without memory, $E(\mathcal{TB}(\mathcal{G}))$, and the egalitarian network $\tilde{\mathcal{G}}$, $E(\mathcal{TB}(\tilde{\mathcal{G}}))$, can be bounded as follows using the convexity augment as $t(\tilde{\mathcal{G}}) = t(\mathcal{G})$

$$\begin{aligned}E(\mathcal{TB}(\mathcal{G})) &= N(\mathcal{G}) E\left(\sum_{k=1}^{t(\mathcal{G})} \mathcal{B}(\mathrm{s}_q[k])\right) \\ &\ge N(\mathcal{G}) \left\lceil \log_2\left(\frac{|\max_i(\mathrm{s}_{q_i}[1])| + |\min_i(\mathrm{s}_{q_i}[1])|}{\Delta} + 1\right)\right\rceil \\ &\quad + N(\mathcal{G})(t(\mathcal{G}) - 1)\left\lceil \log_2\left(\frac{|\hat{c}|}{\Delta} + 1\right)\right\rceil\end{aligned} \tag{47}$$

$$\begin{aligned}E(\mathcal{TB}(\tilde{\mathcal{G}})) &= N(\tilde{\mathcal{G}}) E\left(\sum_{k=1}^{t(\mathcal{G})} \mathcal{B}(\mathrm{s}_q[k])\right) \\ &\ge N(\tilde{\mathcal{G}}) \left\lceil \log_2\left(\frac{|\max_i(\mathrm{s}_{q_i}[1])| + |\min_i(\mathrm{s}_{q_i}[1])|}{\Delta} + 1\right)\right\rceil \\ &\quad + N(\tilde{\mathcal{G}})(t(\mathcal{G}) - 1)\left\lceil \log_2\left(\frac{|\hat{c}|}{\Delta} + 1\right)\right\rceil.\end{aligned} \tag{48}$$

In order to find the lower bound on the saving of transmission load using the equipment of memory, let us find an upper bound on the total transmission load for an MLMG network equipped with memory. The transmission load at each time k is considered the largest number of bits to the information transmitted at k. The expected total number of bits transmitted for network $\mathcal{G}$ equipped with memory, denoted as $E(\mathcal{TBM}(\mathcal{G}))$, can be bounded as

$$\begin{aligned}E(\mathcal{TBM}(\mathcal{G})) &= N(\mathcal{G}) E\left(\sum_{k=1}^{t(\mathcal{G})} \max\left(\mathcal{B}(\mathrm{s}_t[k]), \mathcal{B}(\mathrm{v}_t[k])\right)\right) \\ &\le N(\mathcal{G}) \left\lceil \log_2\left(\frac{|\max_i(\mathrm{s}_{t_i}[1])| + |\min_i(\mathrm{s}_{t_i}[1])|}{\Delta} + 1\right)\right\rceil \\ &\quad + N(\mathcal{G}) E\left(\sum_{k=2}^{t(\mathcal{G})} \left\lceil \log_2\left(\frac{2\max(||\mathrm{s}_t[k]||, ||\mathrm{v}_t[k]||)}{\Delta} + 1\right)\right\rceil\right)\end{aligned} \tag{49}$$

The lower bound on the saving of transmission load using the equipment of memory compared to the MLMG and the original egalitarian structures can be calculated through subtracting the lower bounds in (48) and (47) with the upper bounds (49), respectively.

VI. Simulation Studies

In this section, we illustrate results in this paper through simulation studies. Consider the MLMG structure shown in Fig. 2 with four VFCs and three sensor nodes in each group, that is, $m = 4, p = 3$. The FCs form a complete graph [as shown in Fig. 2(a)]. The MLMG topology matrix is described by

$$H = \begin{bmatrix} 1 & 1 & 1 & 1 & 0 & 0 & 1 & 0 & 0 & 1 & 0 & 0 \\ 1 & 0 & 0 & 1 & 1 & 1 & 1 & 0 & 0 & 1 & 0 & 0 \\ 1 & 0 & 0 & 1 & 0 & 0 & 1 & 1 & 1 & 1 & 0 & 0 \\ 1 & 0 & 0 & 1 & 0 & 0 & 1 & 0 & 0 & 1 & 1 & 1 \end{bmatrix}.$$

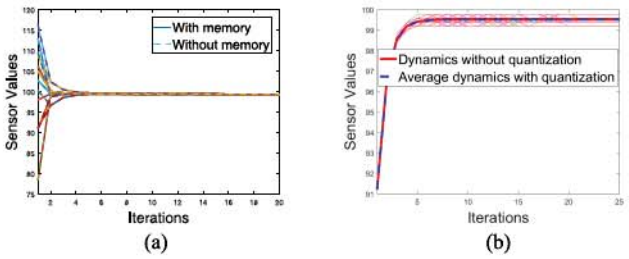

Fig. 4. (a) Comparison of consensus dynamics for one sample run between the cases with and without memories. The dashed lines represent sensor values without memory, and the solid lines represent sensor values with memory. (b) Trajectories of sensor values with quantization for node 5 are denoted with thin lines of different colors representing different sample runs. The expected trajectory of sensor node 5 (dashed blue line) matches the trajectory without quantization (red solid line).

Let the initial value be randomly generated according to a Gaussian random distribution with mean 100 and variance 10. The final consensus value is $\hat{c} = 101.7439$ according to the simulation, which matches the value calculated according to $\frac{1}{\mathbf{1}_{1\times m} H \mathbf{1}_{n\times 1}} \mathbf{1}_{1\times m} H \mathrm{x}[1]$ of Lemma 1. Furthermore, structural results such as that in Lemma 3 directly leads to $\lambda_2 = \frac{1}{3}$ and the upper bound of expected consensus time $t(\mathcal{G}_{\text{comp}}) = \log_{\frac{1}{3}}\left(\frac{\delta}{2}\right)$. By Theorem 5, $N(\mathcal{G}_{\text{comp}}) = 2(p+m-1)m = 48$, and $N(\tilde{\mathcal{G}}_{\text{comp}}) = [m(pm-1) + (p-1)m(p+m-2)] = 84$.

Using the probabilistic quantization algorithm (3) and (4), the solid lines in Fig. 4(a) shows the trajectory of all sensor nodes in one sample run, $\mathrm{s}[k]$. A 10-b quantizer is used to code data for the channel transmissions. Cearly, consensus is reached according to Theorem 1. Note that each sample run may not have the same dynamics, and the final consensus value may be different from $\hat{c}$. This is also clear from Fig. 4(b), which shows 1000 sample runs for one sensor node (node 5 in particular). Clearly, in spite of the variability of each sample run, the expected trajectory matches precisely the trajectory without quantization (shown in dashed blue line). The expected final consensus value for each of the sensor nodes is also $\hat{c}$ according to Theorem 2.

The employment of memory (6) and (7) does not change sensor values, as $\mathrm{s}_m[k] = \mathrm{s}[k]$ according to Theorem 7. This equivalence can be seen clearly from the dashed lines in Fig. 4(a), which overlap with the solid lines for the dynamics without memories.

Now we study the transient bounds. We show the bounds of $E(\mathrm{s}_q[k]) - \hat{s}\mathbf{1}$ in Fig. 5(a), which verifies Theorems 3 and 7. The plot for $E(\mathcal{Q}(\mathrm{s}_m[k]))$ is the same and, hence, is omitted. Fig. 5(b) shows the expected transient bounds of the transmitted sensor values, $E(\mathrm{s}_t[k])$, according to Corollary 3. Fig. 5(c) and (d) show the bounds for the expected ranges of quantized sensor values without memory $E(\overline{\mathrm{s}_q}[k])$ (see Theorem 4) and the quantized sensor values to send in the presence of memory $E(\overline{\mathrm{s}_t}[k])$ (see Corollary 3).

Here, we compare the total transmission load needed to reach consensus for three schemes. Purely distributed egalitarian structure $\tilde{\mathcal{G}}$, MLMG structure $\mathcal{G}$ without memory, and MLMG structure $\mathcal{G}$ with memory. Assume that $\delta = 0.001$ and, hence, $t(\mathcal{G}) = 10$. The transmission loads and their bounds are

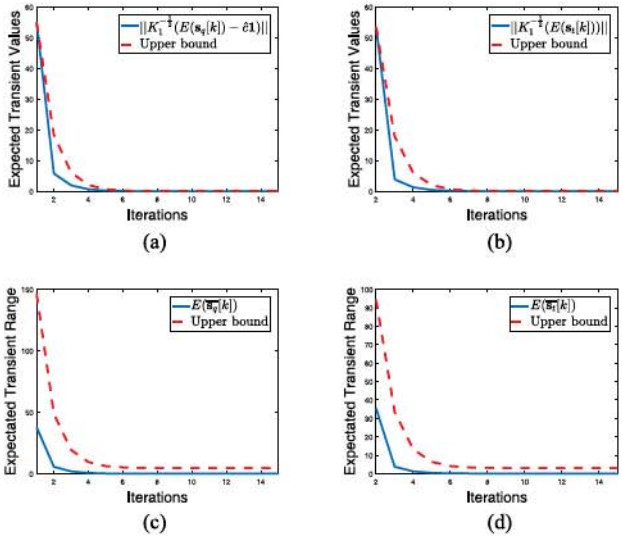

Fig. 5. (a) Transient performance of the case without additional memories: upper bound of the scaled norm difference between expected sensor values and the final consensus value. (b) Transient performance of the case with additional memories: Upper bound of scaled expected sensor values to be transmitted. (c) Upper bound of the expected range of sensor values without memory (d) Upper bound of the expected range of sensor values to be transmitted with the employment of additional memories.

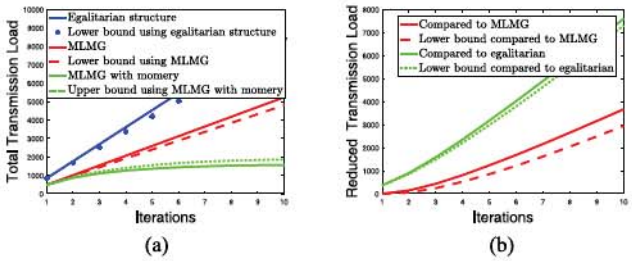

Fig. 6. (a) Total transmission loads and their bounds for three schemes. (b) Reduced total transmission loads and their lower bounds through using MLMG and the employment of memories.

shown in Fig. 6(a). Through employing local memories, the total transmission load converges with growing correlations among sensor values. Fig. 6(b) shows the lower bounds on the transmission loads that can be saved by using the use of local memories, compared to the MLMG and the equivalent egalitarian structures.

VII. Concluding Remarks and Future Work

Using a structural approach, we showed that layered structures with the installation of additional memories can significantly reduce data transmission load, making this structure promising for UAV networks. We proved the asymptotic and transient properties of the memory-based quantized consensus, and linked these properties to simple graphical characteristics of the MLMG structures. In the future work, we will introduce mobility to the framework and study distributed computing tasks for UAV networks under random topology variations.

ACKNOWLEDGMENT

We thank Dr. S. Fu and Dr. J. Xie for valuable discussions made for the conference version.

REFERENCES

[1] FAA, Press Release—DOT and FAA Finalize Rules for Small Unmanned Aircraft Systems, 2016. [Online]. Available: https://www.faa.gov/news/press_releases/news_story.cfm?newsId=20515

[2] X. Meng, W. Wang, and B. Leong, "SkyStitch: Cooperative multi-UAV-based real-time video surveillance system with stiching," in *Proc. 23rd ACM Int. Conf. Multimedia*, 2015, pp. 261–270.

[3] D. W. Casbeer, "Cooperative fire monitoring using multiple UAVs," *Distributed Consensus in Multi-Vehicle Cooperative Control*, W. Ren and R. W. Beard, Eds. Berlin, Germany: Springer-Verlag, 2008, pp. 247–264.

[4] Y. Gu, M. Zhou, S. Fu, and Y. Wan, "Airborne WiFi networks through directional antennae: An experimental study," in *Proc. 2015 IEEE Wireless Commun. Netw. Conf.*, 2015, pp. 1314–1319.

[5] J. Yan, Y. Wan, S. Fu, J. Xie, S. Li, and K. Lu, "RSSI-based decentralized control for robust long-distance aerial networks using directional antennas," *IET Control Theory Appl.*, vol. 11, no. 11, Jul. 2017, pp. 1838–1847.

[6] B. Zhou, L. H. Ngoh, B. S. Lee, and C. P. Fu, "Hda: A hierarchical data aggregation scheme for sensor networks," *Comput. Commun.*, vol. 29, no. 9, pp. 1292–1299, Nov. 2006.

[7] R. Olfati-Saber, J. A. Fax, and R. Murray, "Consensus and cooperation in networked multi-agent systems," *Proc. IEEE*, vol. 95, no. 11, pp. 215–233, Jan. 2007.

[8] R. Wei, R. W. Beard, and E. M. Atkins, "Information consensus in multi-vehicle cooperative control," *IEEE Control Syst.*, vol. 27, no. 2, pp. 71–82, Apr. 2007.

[9] T. Yang, S. Roy, Y. Wan, and A. Saberi, "Constructing consensus controllers for networks with identical general linear agents," *Int. J. Robust Nonlinear Control*, vol. 21, no. 11, pp. 1237–1256, 2011.

[10] Y. Wan, K. Namuduri, S. Akula, and M. Varanasi, "The impact of multi-group network structure on the performance of distributed consensus building strategies," *Int. J. Robust Nonlinear Control*, vol. 23, no. 6, pp. 653–662, Apr. 2013.

[11] T. Lv, H. Gao, X. Li, S. Yang, and L. Hanzo, "Space-time hierarchical-graph based cooperative localization in wireless sensor networks," *IEEE Trans. Signal Process.*, vol. 64, no. 2, pp. 322–334, Jan. 2016.

[12] H. Song, W. A. Zhang, and L. Yu, "Hierarchical fusion in clustered sensor networks with asynchronous local estimates," *IEEE Signal Process. Lett.*, vol. 21, no. 12, pp. 1506–1510, Dec. 2014.

[13] Y. Y. Liu, J. J. Slotine, and A. L. Barabási, "Control centrality and hierarchical structure in complex networks," *Plos One*, vol. 7, no. 9, Sep. 2012, Art. no. e44459.

[14] H. I. Su and A. E. Gamal, "Distributed lossy averaging," *IEEE Trans. Inf. Theory*, vol. 56, no. 7, pp. 3422–3437, Jul. 2010.

[15] M. E. Yildiz and A. Scaglione, "Differential nested lattice encoding for consensus problems," in *Proc. ACM Int. Symp. Inf. Process. Sensor Netw*, Apr. 2007, pp. 89–98.

[16] M. E. Yildiz and A. Scaglione, "Coding with side information for rate-constrained consensus," *IEEE Trans. Signal Process.*, vol. 56, no. 8, pp. 3753–3764, Aug. 2008.

[17] A. Nedic, A. Olshevsky, A. Ozdaglar, and J. Tsitsiklis, "On distributed averaging algorithms and quantization effects," *IEEE Trans. Autom. Control*, vol. 54, no. 11, pp. 2506–2517, Nov. 2009.

[18] R. Carli, F. Fagnani, P. Frasca, T. Taylor, and R. Zampieri, "Average consensus on networks with transmission noise or quantization," in *Proc. Eur. Control Conf.*, Jul. 2007, pp. 1852–1857.

[19] R. Carli, P. Frasca, F. Fagnani, and S. Zampieri, "Gossip consensus algorithms via quantized communication," *Automatica*, vol. 46, no. 1, pp. 70–80, Jan. 2010.

[20] R. Carli, F. Bullo, and S. Zampieri, "Quantized average consensus via dynamic coding/decoding schemes," *Int. J. Robust Nonlinear Control*, vol. 20, no. 2, pp. 156–175, Jan. 2010.

[21] T. Li, M. Fu, L. Xie, and J. Zhang, "Distributed consensus with limited communication data rate," *IEEE Trans. Autom. Control*, vol. 56, no. 2, pp. 279–292, Feb. 2011.

[22] P. Frasca, R. Carli, F. Fagnani, and S. Zampieri, "Average consensus on networks with quantized communication," *Int. J. Robust Nonlinear Control*, vol. 19, no. 16, pp. 1787–1816, Nov. 2009.

[23] T. C. Aysal, M. Coates, and M. Rabbat, "Distributed average consensus with dithered quantization," *IEEE Trans. Signal Process.*, vol. 56, no. 10, pp. 4905–4918, Oct. 2008.

[24] T. C. Aysal, M. J. Coates, and M. G. Rabbat, "Rates of convergence of distributed average consensus using probabilistic quantization," in *Proc. Allerton Conf. Commun., Control Comput.*, Sep. 2007, pp. 1–8.

[25] A. Censi and R. Murray, "Real-valued consensus over noisy quantized channels," in *Proc. Amer. Control Conf.*, Jun. 2009, pp. 4361–4366.

[26] S. Kar and J. M. F. Moura, "Distributed consensus algorithms in sensor networks: quantized data and random link failures," *IEEE Trans. Signal Process.*, vol. 58, no. 3, pp. 1383–1400, Mar. 2010.

[27] A. Kashyap, T. Basar, and R. Srikant, "Quantized consensus," *Automatica*, vol. 43, no. 7, pp. 1192–1203, Jul. 2007.

[28] S. Zhu and B. Chen, "Distributed average consensus with deterministic quantization: An ADMM approach," in *Proc. IEEE Global Conf. Signal Inf. Process.*, Dec. 2015, pp. 692–696.

[29] J. Lavaei and R. M. Murray, "Quantized consensus by means of gossip algorithm," *IEEE Trans. Autom. Control*, vol. 57, no. 1, pp. 19–32, Jan. 2012.

[30] R. Carli, P. Frasca, F. Fagnani, and S. Zampieri, "Gossip consensus algorithms via quantized communication," *Automatica*, Jan. 2010, pp. 70–80.

[31] S. Zhu and B. Chen, "Quantized consensus by the ADMM: Probabilistic versus deterministic quantizers," *IEEE Trans. Signal Process.*, vol. 64, no. 7, pp. 1700–1713, Apr. 1, 2016.

[32] K. Cai and H. Ishii, "Quantized consensus and averaging on gossip digraphs," *IEEE Trans. Autom. Control*, vol. 56, no. 9, pp. 2087–2100, Sep. 2011.

[33] D. Li, Q. Liu, X. Wang, and Z. Lin, "Consensus seeking over directed networks with limited information communication," *Automatica*, vol. 49, no. 2, pp. 610–618, Feb. 2013.

[34] L. P. Devroye, "Inequalities for the completion times of stochastic PERT networks," *Math. Oper. Res.*, vol. 4, no. 4, pp. 441–447, Nov. 1979.

[35] V. Sheth, Y. Wan, J. Xie, S. Fu, Z. Lin, and S. K. Das, "On properties of quantized consensus in multi-layer multi-group sensor networks," in *Proc. IEEE Int. Conf. Distrib. Comput. Sensor Syst.*, Marina Del Rey, CA, USA, May 26–28, 2014, pp. 217–224.

Yan Wan (SM'17) received the Ph.D. degree in electrical engineering from Washington State University, Pullman, WA, USA, in 2009.

She is currently an Associate Professor with the Electrical Engineering Department, University of Texas at Arlington, Arlington, TX, USA. She had her postdoctoral training at the University of California, Santa Barbara, Santa Barbara, CA, USA. From 2009 to 2016, she was an Assistant Professor and then an Associate Professor with the University of North Texas, Denton, TX, USA. Her research has led to more than 130 publications and successful technology transfer outcomes. Her research interests include modeling, evaluation and control of large-scale dynamical networks, cyber-physical system, stochastic networks, decentralized control, learning control, networking, uncertainty analysis, algebraic graph theory, and their applications to UAV networking, UAV traffic management, epidemic spread, complex information networks, and air traffic management.

Dr. Wan is recognized by several prestigious awards, including the NSF CAREER Award, RTCA William E. Jackson Award, and the U.S. Ignite and GENI demonstration awards. She is currently the Vice President of the IEEE Comsoc Fort Worth Chapter and Technical Committee Member of AIAA Intelligent Systems Society. She is also the Associate Editor for the *Transactions of the Institute of Measurement and Control.*

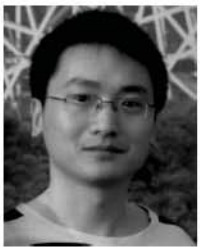

Jing Yan (M'14) received the B.Eng. degree in automation from Henan University, Kaifeng, China, in 2008, and the Ph.D. degree in control theory and control engineering from Yanshan University, Qinhuangdao, China, in 2014.

In 2014, he was a Research Assistant with the Key Laboratory of System Control and Information Processing, Ministry of Education, Shanghai Jiaotong University, Shanghai, China. In 2016, he was a Research Associate with the University of Texas at Arlington, Arlington, TX, USA. He is currently an Associate Professor with Yanshan University. He has authored more than 20 referred international journal and conference papers. He is the inventor of two patents. His research interests cover in networked teleoperation systems, underwater acoustic sensor networks, and cyberphysical systems.

Dr. Yan was a recipient of the competitive National Graduate Scholarship from the Ministry of Education of China in 2012. He was the recipient of the Excellence Paper Award from the National Doctoral Academic Forum of System Control and Information Processing in 2012, and the Science and Technology Innovation Award from Yanshan University in 2013.

Zongli Lin (F'07) received the B.S. degree in mathematics and Computer Science from Xiamen University, Xiamen, China, in 1983, the Master's of Engineering degree in automatic control from Chinese Academy of Space Technology, Beijing, China, in 1989, and the Ph.D. degree in electrical and computer engineering from Washington State University, Pullman, WA, USA, in 1994.

He is currently the Ferman W. Perry Professor with the School of Engineering and Applied Science and a Professor of Electrical and Computer Engineering with the University of Virginia, Charlottesville, VA, USA. His current research interests include nonlinear control, robust control, and control applications.

Dr. Lin was an Associate Editor of the IEEE TRANSACTIONS ON AUTOMATIC CONTROL (2001–2003), the IEEE/ASME TRANSACTIONS ON MECHATRONICS (2006–2009), and the IEEE CONTROL SYSTEMS MAGAZINE (2005–2012). He was an elected member of the Board of Governors of the IEEE Control Systems Society (2008–2010) and chaired the IEEE Control Systems Society Technical Committee on Nonlinear Systems and Control (2013–2015). He was on the operating committees of several conferences and is the program chair of the 2018 American Control Conference and a general chair of the 16th International Symposium on Magnetic Bearings, 2018. He is currently on the editorial boards of several journals and book series, including Automatica, Systems and Control Letters, and Springer/Birkhauser book series Control Engineering. He is a Fellow of the IFAC, and a Fellow of AAAS, the American Association for the Advancement of Science.

Vardhman Sheth received the B.S. degree in electronics and telecommunications from the Savitribai Phule Pune University, Pune, India, in 2011 and the Master's degree in electrical engineering from the University of North Texas, Denton, TX, USA, in 2014.

He is currently the Algorithms and Systems Lead with Linear Dimensions, San Jose, CA, USA. His research interests include embedded systems, robotics, signal processing, and machine learning.

Sajal K. Das (F'15) received the Ph.D. degree in computer science from the University of Central Florida in 1988. He is a professor of Computer Science and the Daniel St. Clair Endowed Chair with the Missouri University of Science and Technology, Rolla, MO, USA. He has authored or coauthored extensively in these areas with more than 700 research articles in high-quality journals and refereed conference proceedings. He holds five U.S. patents and coauthored four books. His h-index is 79 with more than 25 500 citations according to Google Scholar. His research interests include theory and practice of wireless sensor networks, cyber physical systems, smart environments (smart city, smart grid, and smart health care), and cloud computing, big data analytics, IoT, cyber-physical security, biological and social networks, applied graph theory and game theory.

Mr. Das is a recipient of ten Best Paper Awards at prestigious conferences such as ACM MobiCom and IEEE PerCom, and numerous awards for teaching, mentoring, and research including the IEEE Computer Societys Technical Achievement Award for pioneering contributions to sensor networks and mobile computing. He is the Founding Editor-in-Chief of the Pervasive and Mobile Computing Journal since 2005, and Associate Editor of the IEEE TRANSACTIONS OF MOBILE COMPUTING and the *ACM Transactions on Sensor Networks*.